Applied Mathematical Modelling 61 (2018) 618–633

Contents lists available at ScienceDirect

Applied Mathematical Modelling

journal homepage: www.elsevier.com/locate/apm

Free vibration analysis of dowelled rectangular isotropic thin plate on a Modified Vlasov soil type by using discrete singular convolution method

Mohamed Gibigaye[a,*], Crespin Prudence Yabi[a], Gerard Degan[b]

[a] University of Abomey-Calavi, 01BP 2009 Cotonou, Benin
[b] National University of Sciences, Technologies, Engineering and Mathematics, BP: 2282 Goho-Abomey, Benin

ARTICLE INFO

Article history:
Received 18 December 2017
Revised 18 April 2018
Accepted 15 May 2018
Available online 24 May 2018

Keywords:
Free vibration
Semi-rigid boundary conditions
DSC method
Taylor series expansion
Modified Vlasov soil
Thin isotropic plate

ABSTRACT

The behaviour of plates resting on elastic foundations has wide interest because it is an important model for many engineering applications. Natural frequencies and corresponding mode shapes are guides to investigating the behaviour of a soil-structure system with time. Therefore, free vibration analysis constitutes a considerable part of research done on this topic. In this study, the effects of the stiffness of a surrounding Modified Vlasov soil type, the soil depth, and the aspect ratio on the free vibration of a thin rectangular dowelled plate on the Modified Vlasov soil type are investigated. We used a discrete singular convolution (DSC) with a Taylor series expansion method to apply the boundary conditions. The two formulas of the Taylor series expansion are used in the DSC to eliminate the fictitious points outside the physical domain. It is noticed that beyond a certain depth, neither the effective depth of the soil nor the, frequency varies consistently. Furthermore, the dynamically activated depth influences the frequency values for plates more than for beams. In addition, the effect of the elastic rotational stiffness of the surrounding soil is found to be negligible compared to that of the elastic vertical translational one. The results obtained can serve as a basis for the dynamic analysis of rigid pavements.

Published by Elsevier Inc.

1. Introduction

Plates are important components of engineering structures; therefore, the vibration analysis of thin rectangular plates is a significant subject in engineering procedure [1]. The behaviour of plates resting on elastic foundations has a wider interest because it is an important model for many engineering applications. Natural frequencies and corresponding mode shapes are guides to investigate the behaviour of a soil-structure system with time [2]. Therefore, free vibration analysis constitutes a considerable part of research done on this topic. For rectangular plates, the semi-rigidity in the boundary conditions refers to many civil and mechanical systems, such as dowel and tie bars, in engineering practice [3,4]. Many studies have been performed on the vibration of such plates [4–7]. As analytical solutions are only available for certain cases of boundary conditions, numerical methods are the major approach in this research field [8]. To analyse plates with semi-rigid boundary conditions (mainly dowelled thin isotropic plates), many numerical approaches exist [9]: the Modified Bolotin Method [3], its further modification [7], the Fourier spectral method [5,10], the differential quadrature method [11–17], the finite

* Corresponding author.
E-mail addresses: mohamed.gibigaye@uac.bj (M. Gibigaye), yabicrespin@gmail.com (C.P. Yabi), ger_degan@yahoo.fr (G. Degan).

https://doi.org/10.1016/j.apm.2018.05.019
0307-904X/Published by Elsevier Inc.

element-differential quadrature method [9,18], the upper bound method [19], and the discrete singular convolution (DSC) proposed by Wei and co-workers [10,20,21]. These methods are accurate for lower modes, while for higher modes, the DSC method is one of the latest and most accurate without loss of performance for lower modes [1,8,22,23].

Owing to the high accuracy of the DSC method, many researchers worked toward extending its application field [8,13,20,24]. Based on distribution theories, the DSC method was proposed by Wei in 1999 [25] and has been successfully used to analyse the static, vibration, and buckling of beams, plates, and shells [26]. However, implementation of the boundary conditions by strong form methods such as the DSC method is a difficult but important task. The major problem of the DSC method is the presence of fictitious points that increase the number of unknown parameters. Some methods permit the transformation of the fictitious points to inner points, such as the method of symmetric extension (used to apply clamped boundary conditions) and the method of anti-symmetric extension (used to apply simply supported boundary conditions) [20,27,28]. However, these two methods cannot be used to apply free, semi-rigid, or general boundary conditions, and can be only used for simple or mixed boundary conditions [8,24,29].

Therefore, Wang and co-workers introduced the Taylor series expansion to apply free-edge boundary conditions to thin isotropic and anisotropic plates [1,24]. The authors concluded that this method is more accurate than earlier approaches [29]. However, this method neglects the degree of freedom of mixed derivatives, thus causing some accuracy and instability problems. To solve these problems, Wang and Yuan [8] proposed one condition for each corner of a rectangular plate to avoid the free-corner conditions. This study demonstrated that the Taylor series expansion method to apply boundary conditions is general, accurate, and can be used for arbitrary boundary conditions.

In addition, there are many studies on the free vibrations of a plate resting on an elastic Winkler soil type [30], Pasternak soil type [31,32], or Vlasov soil type [2]. For these types of soils, elastic parameters such as the reaction modulus k_O, shear modulus c_O, and logarithmic decrement γ are usually considered empirically or arbitrarily. This can induce imprecisions in the appreciation of the state of stress and the deformation of the plate-soil system. To make the analysis of the free vibrations of the plate more precise, the elastic parameters of the soil should also be determined more precisely. To do this, the Modified Vlasov soil type performs better than other types [4,33]. However, the Modified Vlasov soil type requires the following to be taken into account: the rigidities of the soil surrounding the plate and the vertical translation and rotation rigidities in the equations related to the boundary conditions [33]. Therefore, a study of the Modified-Vlasov-soil-type foundation requires the consideration of semi-rigid boundary conditions for the plate. This case of boundary conditions has not yet been explicitly taken into account in previous studies [1,8,24] when using the DSC method.

This study investigates the effects of the stiffness of the surrounding soil, aspect ratio, and subsoil depth on the frequency parameter of a thin rectangular dowelled plate of the Modified Vlasov soil type. To do this, we extended the application of the Taylor series approach to a free vibration analysis of the dowelled rectangular plate, with all edges elastically restrained, using the DSC method. This system, modelling a rigid pavement, is useful in pavement design, and especially in its dynamic analysis.

2. Modelling the plate-soil system

Consider the free vibration of a thin isotropic rectangular plate with length a, width b, and thickness h, resting on a Modified Vlasov soil foundation. This is shown in Fig. 1. According to the classic theory of thin plates, and taking into account the reduced mass of the soil, the transverse deflection of the Kirchhoff plate satisfies the following partial differential equation [4]:

$$D\nabla^4 \mathrm{w}(x,y,t) + k_o \mathrm{w}(x,y,t) - C_o\nabla^2 \mathrm{w}(x,y,t) = (\rho h + m_o)\frac{\partial^2 \mathrm{w}(x,y,t)}{\partial t^2}, \tag{1}$$

where $\mathrm{w}(x,y,t) = \bar{w}(x,y,0,t)$, meaning that the deflection of the Kirchhoff plate is equal to the deflection of the plate/soil interface. $\bar{w}(x,y,z,t)$ is the deflection at the plate/soil interface and is defined as $\bar{w}(x,y,z,t) = \bar{w}(x,y,0,t)\phi(z)$. $\phi(z) = \sinh[\gamma(1-\frac{z}{H_S})]/\sinh\gamma$ is a vertical decay function of soil that must verify $\phi(0) = 1$ and $\phi(H_s) = 0$.

$\bar{w}(x,y,z,t)$ is the deflection inside the soil layer.

$D = Eh^3/[12(1-\upsilon^2)]$ is the flexural rigidity of the plate; k_O is the modulus of the reaction or the integral characteristic in the compression of the soil; $C_o = 2c_o$ where c_o is the shearing modulus or the integral characteristic in the shearing of the soil; and m_O is the linear reduced mass of the foundation soil, assuming it is homogeneous and monolayered. This is expressed as follows [4]:

$$k_o = \frac{E_o}{1-\upsilon_0{}^2}\int_0^{H_S}\left[\phi'(z)\right]^2 dz = \frac{E_o}{2H_S(1-\upsilon_o{}^2)}\frac{\gamma(\gamma+\sinh\gamma\cosh\gamma)}{(\sinh\gamma)^2} \tag{2}$$

$$c_o = \frac{E_o}{4(1+\upsilon_o)}\int_0^{H_S}[\phi(z)]^2 dz = \frac{E_o H_S}{8(1+\upsilon_o)}\frac{(\sinh\gamma\cosh\gamma-\gamma)}{\gamma(\sinh\gamma)^2} \tag{3}$$

$$m_o = m_S\int_0^{H_S}[\phi(z)]^2 dz = \frac{m_S H_S(\sinh\gamma\cosh\gamma-\gamma)}{2\gamma(\sinh\gamma)^2} \tag{4}$$

In Eq. (2)–(4), H_S is the effective finite depth of the foundation that is dynamically activated, m_S is the density of the subgrade, and γ is a constant named as the logarithmic decrement of the soil and determines the rate of decrease

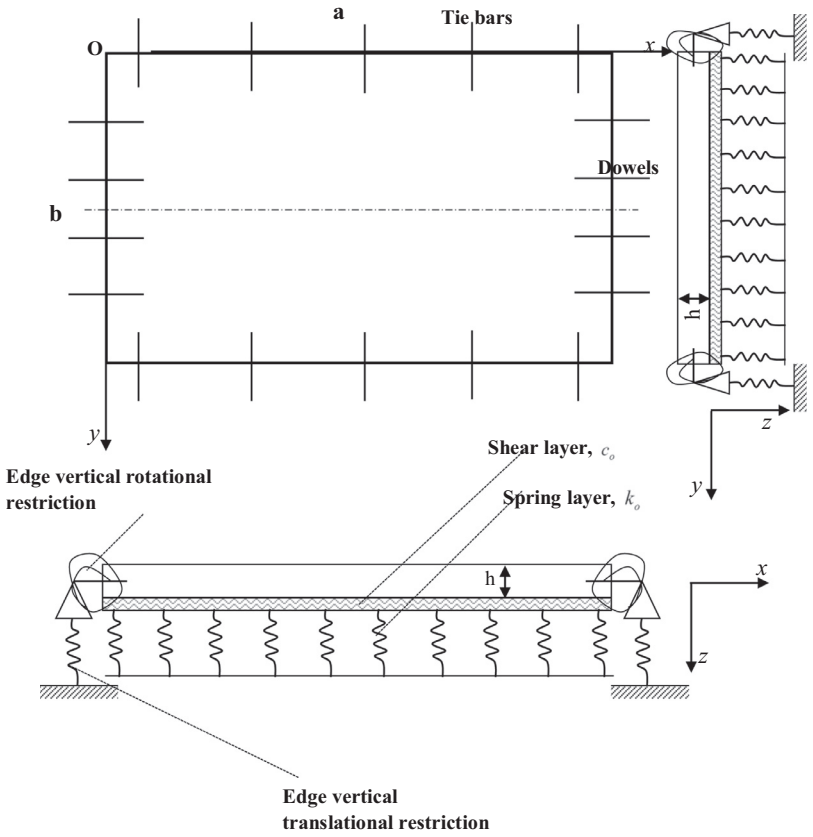

Fig. 1. Modelling of dowelled plate resting on Modified Vlasov soil type.

of the deflections depending on the depth. E_O and υ_O are certain moduli of the soil defined as $E_O = E_S/(1-\upsilon_S^2)$ and $\upsilon_O = \upsilon_S/(1+\upsilon_S)$, where E_S is the Young's modulus of the soil, and υ_S is its Poisson's ratio.

The boundary conditions (Fig. 1) are modelled as follows:

- The restriction of the elastic vertical translation is characterised by four equations [4]:

$$V_{x=0} = -D\left[\frac{\partial^3 w(0,y,t)}{\partial x^3} + (2-\upsilon)\frac{\partial^3 w(0,y,t)}{\partial x \partial y^2}\right] = (ks_{soil} + ks_{x1})w(0,y,t) \tag{5a}$$

$$V_{x=a} = D\left[\frac{\partial^3 w(a,y,t)}{\partial x^3} + (2-\upsilon)\frac{\partial^3 w(a,y,t)}{\partial x \partial y^2}\right] = (ks_{soil} + ks_{x2})w(a,y,t) \tag{5b}$$

$$V_{y=0} = -D\left[\frac{\partial^3 w(x,0,t)}{\partial y^3} + (2-\upsilon)\frac{\partial^3 w(x,0,t)}{\partial y \partial x^2}\right] = \left(ks_{soil} + ks_{y1}\right)w(x,0,t) \tag{5c}$$

$$V_{y=b} = D\left[\frac{\partial^3 w(x,b,t)}{\partial y^3} + (2-\upsilon)\frac{\partial^3 w(x,b,t)}{\partial y \partial x^2}\right] = \left(ks_{soil} + ks_{y2}\right)w(x,b,t) \tag{5d}$$

where ks_{x1},ks_{x2},ks_{y1},ks_{y2} are the elastic vertical translation stiffnesses; V_x,V_y are the vertical shear forces of the plate; and $ks_{soil} = \sqrt{k_O C_O}$ is the elastic vertical translational stiffness owing to the surrounding soil.

- The restriction of the elastic rotation is characterised by the following four equations [14]:

$$M_{x=0} = -D\left[\frac{\partial^2 w(0,y,t)}{\partial x^2} + \upsilon\frac{\partial^2 w(0,y,t)}{\partial y^2}\right] = (kr_{soil} + kr_{x1})\frac{\partial w(0,y,t)}{\partial x} \tag{6a}$$

$$M_{x=a} = D\left[\frac{\partial^2 w(a,y,t)}{\partial x^2} + \upsilon\frac{\partial^2 w(a,y,t)}{\partial y^2}\right] = (kr_{soil} + kr_{x2})\frac{\partial w(a,y,t)}{\partial x} \tag{6b}$$

$$M_{y=0} = -D\left[\frac{\partial^2 w(x,0,t)}{\partial y^2} + \upsilon\frac{\partial^2 w(x,0,t)}{\partial x^2}\right] = \left(kr_{soil} + kr_{y1}\right)\frac{\partial w(x,0,t)}{\partial y} \tag{6c}$$

$$M_{y=b} = D\left[\frac{\partial^2 w(x,b,t)}{\partial y^2} + \upsilon\frac{\partial^2 w(x,b,t)}{\partial x^2}\right] = \left(kr_{soil} + kr_{y2}\right)\frac{\partial w(x,b,t)}{\partial y} \tag{6d}$$

where kr_{x1},kr_{x2},kr_{y1},kr_{y2} are the elastic rotational stiffnesses; M_x,M_y are the bending moments of the finite plate; and $kr_{soil} = 1/2(C_O\sqrt{C_O/k_O})$ is the elastic rotational stiffness owing to the surrounding soil.

- The restriction of the elastic torsion at the four corners of the plate is characterised by four equations:

$$M_{xy} = -D(1-\upsilon)\frac{\partial^2 w(x,y,t)}{\partial x \partial y} = (kxy_{soil} + k_{xy})w(x,y,t) \tag{6e}$$

where $(x;\ y)$ are $\{(x=0;\ y=0);\ (x=0;\ y=b);\ (x=a;\ y=0);\ (x=a;\ y=b)\}$; M_{xy} is the torsional moment of the finite plate; $kxy_{soil} = 3C_O/4$, the elastic torsional stiffness at each corner of the plate owing to the effect of the surrounding soil; and k_{xy} is the elastic torsional stiffness at each corner of the plate.

For generality and simplicity, the following dimensionless parameters are introduced for a rectangular $(a \times b)$ plate:

$$X = \frac{x}{a}, Y = \frac{y}{b}, W = \frac{w}{a}; \beta = \frac{a}{b}; Kr = \frac{k_O.a^4}{D}; Cr = \frac{C_O.a^2}{D}; \Omega = \omega a^2\sqrt{\frac{\rho h + m_O}{D}} \tag{7}$$

where ω is the natural frequency of the plate.

Thus, the governing equation for the free vibration of a plate in Eq. (1) can be expressed in the dimensionless form as

$$\frac{\partial^4 W}{\partial X^4} + 2\beta^2\frac{\partial^4 W}{\partial X^2 \partial Y^2} + \beta^4\frac{\partial^4 W}{\partial Y^4} + Kr.W + Cr.\left(\frac{\partial^2 W}{\partial X^2} + \beta^2\frac{\partial^2 W}{\partial Y^2}\right) = \Omega^2 W \tag{8}$$

here, $W = W(X, Y, t)$.

3. Discrete singular convolution and solution procedures

The DSC algorithm was adopted to cope with the governing equation and boundary conditions. In the DSC algorithm, the nth -order derivative of a function $W(x)$ is approximated via a discretised convolution [24,34]:

$$w^{(n)}(x) \approx \sum_{k=-M}^{M} \delta_{\sigma,\Delta}^{(n)}(x - x_k)w(x_k) \qquad (n = 1, 2, \ldots) \tag{9}$$

where M is such that $2M+1$ is the computational bandwidth, and x_k $(k = -M,\ldots, -1, 0, 1,\ldots, M)$ are uniformly distributed grid points. Superscripts (n) denote the nth -order derivative with respect to x, $\delta_{\sigma,\Delta}^{(n)}(x - x_k)$ is a collection symbol for the DSC kernels, and its nth-order derivative is given by Civalek and co-workers [23,35]

$$\delta_{\sigma,\Delta}^{(n)}(x - x_k) = \left(\frac{d}{dx}\right)^n \delta_{\sigma,\Delta}(x - x_k), \quad (n = 1, 2, \ldots) \tag{10}$$

There are several Dirichlet-type delta kernels available. The two most widely used are the regularized Shannon kernel (DSC-RSK) and the nonregularised Lagrange's delta sequence kernel (DSC-LK). In this work, the DSC algorithm can be realised using many approximation kernels. However, it was shown that for many problems, the use of an RSK kernel is very efficient [35,36]. In this study, the regularised Shannon's delta sequence kernel (DSC-RSK) [8,36] is employed. The regularised Shannon kernel is defined as [8,24,28]

$$\delta_{\sigma,\Delta}(x - x_k) = \frac{\sin[\pi/\Delta(x - x_k)]}{\pi/\Delta(x - x_k)} exp\left[-\frac{(x - x_k)^2}{2\sigma^2}\right] \tag{11}$$

where σ is a controllable parameter, and $\Delta = x_k - x_{k-1}$ is the spacing between two grid points.

The parameter σ determines the width of the Gaussian envelope and often varies in association with grid spacing $\sigma = r \times \Delta$, where r is a parameter chosen in computation. It is also known that the truncation error is very small owing to the use of a Gaussian regulariser. The above formulation given by Eq. (11) is practically an essential compact support for numerical interpolation [37]. With a sufficiently smooth approximation, it is more effective to consider a discrete singular convolution.

In this study, we considered a uniform grid such as

$$0 = X_0 < X_1 < \cdots < X_N = 1 \text{ and } 0 = Y_0 < Y_1 < \cdots < Y_N = 1 \tag{12}$$

3.1. Taylor series method

The studied plate is dowelled and subjected to the effects of the surrounding soil at its edges. Thus, the boundary conditions are semi-rigid. The well-known symmetric and antisymmetric extension [27,38] cannot easily handle the semi-rigid boundary conditions formulated in Eqs. (5) and (6). Thus, in the present study, we used a method based on the Taylor series expansion as proposed by Wang and Yuan [8] for the case of free-edge boundary conditions.

The Taylor series expansions for $w(x)$ and $w(2x_o - x)$ at $x = x_o$ can be written as

$$\mathrm{w}(x) = \mathrm{w}(x_o) + \mathrm{w}^{(1)}(x_o)(x - x_o) + \frac{1}{2!}w^{(2)}(x_o)(x - x_o)^2 + \frac{1}{3!}w^{(3)}(x_o)(x - x_o)^3 + \frac{1}{4!}w^{(4)}(x_o)(x - x_o)^4 + \frac{1}{5!}w^{(5)}(x_o)(x - x_o)^5 + \ldots \tag{13}$$

$$w(2x_o - x) = w(x_o) - w^{(1)}(x_o)(x - x_o) + \frac{1}{2!}w^{(2)}(x_o)(x - x_o)^2 - \frac{1}{3!}w^{(3)}(x_o)(x - x_o)^3 + \frac{1}{4!}w^{(4)}(x_o)(x - x_o)^4 - \frac{1}{5!}w^{(5)}(x_o)(x - x_o)^5 + \ldots \tag{14}$$

The sum of Eqs. (13) and (14) is more accurate than the difference of Eqs. (13) and (14) if two derivative degrees of freedom are retained [1,8,34,39]. Thus, the sum of Eqs. (13) and (14) is adopted as follows:

$$w(x) + w(2x_o - x) = 2w(x_o) + w^{(2)}(x_o)(x - x_o)^2 + \frac{1}{12}w^{(4)}(x_o)(x - x_o)^4 + \ldots \qquad x > xo \tag{15}$$

or

$$w(2x_o - x) = -w(x) + 2w(x_o) + w^{(2)}(x_o)(x - x_o)^2 + \frac{1}{12}w^{(4)}(x_o)(x - x_o)^4 + \ldots \quad x > xo \tag{16}$$

The derivative terms in Eq. (16) are additional degrees of freedom (DOFs) for the studied plate. Based on references [1,8,24], only one additional fictitious DOF is needed for problems involving a second-order differential equation. Thus,

$$w(2x_o - x) = -w(x) + 2w(x_o) + w^{(2)}(x_o)(x - x_o)^2 \quad x > xo \tag{17}$$

For fourth-order differential equations such as the governing equations of the studied plate, two additional degrees of freedom are needed [1,8]. Therefore, Eq. (16) is reduced to Eq. (18) as follows:

$$w(2x_o - x) = -w(x) + 2w(x_o) + w^{(2)}(x_o)(x - x_o)^2 + \frac{1}{12}w^{(4)}(x_o)(x - x_o)^4 \quad x > xo \tag{18}$$

Eqs. (17) and (18) are used to eliminate the DOFs on the M fictitious points outside the domain of the plate. In this study, we used this approach for the general boundary conditions of dowelled edges of a rectangular plate resting on the Modified Vlasov soil type.

3.2. Free vibration of thin rectangular plates by DSC

Consider the free vibration of a thin isotropic rectangular plate by the DSC method using a Taylor series expansion (DSC-T) to take the boundary conditions into account. We assumed that the edges are semi-rigid. We used the DSC-T approach developed in Section 3.1. We assumed here that the implementation bandwidth $2M+1$ is such that $M+1$ is equal to the number N of the grid points in each direction x and y. After removing all degrees of freedom from the fictitious points by the Taylor series expansion [1,24,40], the weighting coefficients in DSC-T of the nth derivative with respect to x are as follows:

- *Case 1:* For $i = 2, 3, \ldots, N-1$ and $M = N-1$, we have

$$w^{(n)}(x_i) = \sum_{k=i-M}^{i+M} C_{i,k-i}^{(n)} w(x_k) = \sum_{k=i-M}^{0} C_{i,k-i}^{(n)} w(x_k) + \sum_{k=1}^{N} C_{i,k-i}^{(n)} w(x_k) + \sum_{k=N+1}^{i+M} C_{i,k-i}^{(n)} w(x_k) \tag{19}$$

- ***C**ase 2: For $i = 1$ and $M = N-1$, we have*

$$w^{(n)}(x_1) = \sum_{k=1-M}^{1+M} C_{1,k-1}^{(n)} w(x_k) = \sum_{k=1-M}^{0} C_{1,k-1}^{(n)} w(x_k) + \sum_{k=1}^{M+1=N} C_{1,k-1}^{(n)} w(x_k) \tag{20}$$

- *Case 3: For $i = N$ and $M = N-1$, we have*

$$w^{(n)}(x_N) = \sum_{k=N-M}^{N+M} C_{N,k-N}^{(n)} w(x_k) = \sum_{k=1}^{N} C_{N,k-N}^{(n)} w(x_k) + \sum_{k=N+1}^{N+M=2N-1} C_{N,k-N}^{(n)} w(x_k) \tag{21}$$

The determination of the weighting coefficients of the grid points is conducted as follows for each of the three cases above:

- *Case 1:* $i=2, 3,\ldots, N-1$ and $M=N-1$

Considering only the positive k, Eq. (19) gives Eq. (22):

$$w^{(n)}(x_i)=\sum_{k=0}^{M-i}C_{i,-k-i}^{(n)}w(x_{-k})+\sum_{k=1}^{N}C_{i,k-i}^{(n)}w(x_k)+\sum_{k=N+1}^{i+M}C_{i,k-i}^{(n)}w(x_k) \tag{22}$$

Using the Taylor series expansion in Eq. (18), at points x_1 and x_N (edges of the grid), we have

$$\begin{aligned}w^{(n)}(x_i)=&\sum_{k=0}^{M-i}C_{i,-k-i}^{(n)}\left[-w(x_{2+k})+2w(x_1)+w^{(2)}(x_1)(x_{-k}-x_1)^2+\frac{1}{12}w^{(4)}(x_1)(x_{-k}-x_1)^4\right]\\&+\sum_{k=N+1}^{M+i}C_{i,k-i}^{(n)}\left[-w(x_{2N-k})+2w(x_N)+w^{(2)}(x_N)(x_k-x_N)^2+\frac{1}{12}w^{(4)}(x_N)(x_k-x_N)^4\right]\\&+\sum_{k=1}^{N}C_{i,k-i}^{(n)}w(x_k)\end{aligned} \tag{23}$$

As $(x_1-x_{-k})=(x_{2+k}-x_1)$ and $(x_N-x_k)=(x_{2N-k}-x_N)$ for a uniform grid,

$$\begin{aligned}w^{(n)}(x_i)=&\sum_{k=0}^{M-i}C_{i,-k-i}^{(n)}\left[-w(x_{2+k})+2w(x_1)+w^{(2)}(x_1)(x_{2+k}-x_1)^2+\frac{1}{12}w^{(4)}(x_1)(x_{2+k}-x_1)^4\right]\\&+\sum_{k=N+1}^{M+i}C_{i,k-i}^{(n)}\left[-w(x_{2N-k})+2w(x_N)+w^{(2)}(x_N)(x_{2N-k}-x_N)^2+\frac{1}{12}w^{(4)}(x_N)(x_{2N-k}-x_N)^4\right]\\&+\sum_{k=1}^{N}C_{i,k-i}^{(n)}w(x_k)\end{aligned} \tag{24}$$

By performing the appropriate index translations, we obtained

$$\begin{aligned}w^{(n)}(x_i)=&\sum_{k=2}^{2+M-i}-C_{i,2-k-i}^{(n)}w(x_k)+\sum_{k=2}^{2+M-i}2C_{i,2-k-i}^{(n)}w(x_1)+\sum_{k=2}^{2+M-i}C_{i,2-k-i}^{(n)}(x_k-x_1)^2w^{(2)}(x_1)\\&+\sum_{k=2}^{2+M-i}\frac{1}{12}C_{i,2-k-i}^{(n)}(x_k-x_1)^4w^{(4)}(x_1)+\sum_{k=1}^{N}C_{i,k-i}^{(n)}w(x_k)+\sum_{k=2N-M-i}^{N-1}-C_{i,2N-k-i}^{(n)}w(x_k)\\&+\sum_{k=2N-M-i}^{N-1}2C_{i,2N-k-i}^{(n)}w(x_N)+\sum_{k=2N-M-i}^{N-1}C_{i,2N-k-i}^{(n)}(x_k-x_N)^2w^{(2)}(x_N)\\&+\sum_{k=2N-M-i}^{N-1}\frac{1}{12}C_{i,2N-k-i}^{(n)}(x_k-x_N)^4w^{(4)}(x_N)\end{aligned} \tag{25}$$

Thus, as proposed in [8], we can write

$$\begin{aligned}w^{(n)}(x_i)&=\sum_{k=1}^{N}F_{i,k}^{(n)}w(x_k)+F_{i,N+1}^{(n)}w^{(2)}(x_1)+F_{i,N+2}^{(n)}w^{(4)}(x_1)+F_{i,N+3}^{(n)}w^{(2)}(x_N)+F_{i,N+4}^{(n)}w^{(4)}(x_N)\\w^{(n)}(x_i)&=\sum_{k=1}^{N}\widetilde{F}_{i,k}^{(n)}\widetilde{w}(x_k)\end{aligned} \tag{26}$$

where

$$F_{i,k}^{(n)}=\begin{cases}C_{i,k-i}^{(n)}+\sum_{j=2}^{2+M-i}2C_{i,2-j-i}^{(n)} & k=1\\ C_{i,k-i}^{(n)}-C_{i,2-k-i}^{(n)} & 2\le k<2+M-i\\ C_{i,k-i}^{(n)}-C_{i,2-k-i}^{(n)}-C_{i,2N-k-i}^{(n)} & k=2+M-i=2N-M-i\\ C_{i,k-i}^{(n)}-C_{i,2N-k-i}^{(n)} & 2N-M-i<k\le N-1\\ C_{i,k-i}^{(n)}+\sum_{j=2N-M-i}^{N-1}2C_{i,2N-j-i}^{(n)} & k=N\end{cases} \tag{27}$$

$$F_{i,N+1}^{(n)}=\sum_{k=2}^{2+M-i}C_{i,2-k-i}^{(n)}(x_k-x_1)^2$$

$$F_{i,N+2}^{(n)} = \sum_{k=2}^{2+M-i} \frac{1}{12} C_{i,2-k-i}^{(n)} (x_k - x_1)^4$$

$$F_{i,N+3}^{(n)} = \sum_{k=2N-M-i}^{N-1} C_{i,2N-k-i}^{(n)} (x_k - x_N)^2$$

$$F_{i,N+4}^{(n)} = \sum_{k=2N-M-i}^{N-1} \frac{1}{12} C_{i,2N-k-i}^{(n)} (x_k - x_N)^4 \tag{28}$$

$F_{i,j}^{(n)}$ are the weighting coefficients of the nth -order derivative with respect to x at point$x_i = (i-1)\Delta x$, N is the number of grid points $\Delta x = 1/(N-1)$, and $\tilde{w}$ is apparent. The variables are considered dimensionless.

- *Case 2:* $i = 1$ and $M = N - 1$.

By proceeding in a similar way as the previous case 1 and using Eq. (20) instead of Eq. (19), the weighting coefficients in Eq. (26) can be rewritten as

$$F_{1,k}^{(n)} = \begin{cases} C_{1,k-1}^{(n)} + \sum_{j=2}^{M+1=N} 2C_{1,2-j-1}^{(n)} & k = 1 \\ C_{i,k-i}^{(n)} - C_{1,2-k-1}^{(n)} & 2 \le k < M+1 = N \end{cases} \tag{29}$$

$$F_{i,N+1}^{(n)} = \sum_{k=2}^{2+M-i} C_{i,2-k-i}^{(n)} (x_k - x_1)^2$$

$$F_{i,N+2}^{(n)} = \sum_{k=2}^{2+M-i} \frac{1}{12} C_{i,2-k-i}^{(n)} (x_k - x_1)^4$$

$$F_{i,N+3}^{(n)} = 0$$

$$F_{i,N+4}^{(n)} = 0 \tag{30}$$

All parameters are defined above.

- *Case 3:* $i = N$ *and* $M = N - 1$.

By proceeding in a similar way as the previous case 1 and using Eq. (21) instead of Eq. (19), the weighting coefficients in Eq. (26) can be rewritten as

$$F_{N,k}^{(n)} = \begin{cases} C_{N,k-i}^{(n)} - C_{N,N-k}^{(n)} & 1 \le k < N-1 \\ C_{N,k-N}^{(n)} + \sum_{j=N-M=1}^{N-1} 2C_{N,N-j}^{(n)} & k = N \end{cases} \tag{31}$$

$$F_{i,N+1}^{(n)} = 0$$

$$F_{i,N+2}^{(n)} = 0$$

$$F_{i,N+3}^{(n)} = \sum_{k=2N-M-i}^{N-1} C_{i,2N-k-i}^{(n)} (x_k - x_N)^2$$

$$F_{i,N+4}^{(n)} = \sum_{k=2N-M-i}^{N-1} \frac{1}{12} C_{i,2N-k-i}^{(n)} (x_k - x_N)^4 \tag{32}$$

All parameters are defined above.

For free vibration analysis of thin rectangular plates by the DSC, the approach presented above can be directly employed with a tensor product once the weighting coefficients in one dimension, Eq. (26), are known.

In terms of DSC, Eq. (8) at all grid points can be expressed as

$$\sum_{k=1}^{Nx+4} D_{i,k}^x \widetilde{W}_{kj} + 2\beta^2 \sum_{k=1}^{Nx+4} \sum_{l=1}^{Ny+4} B_{i,k}^x B_{j,l}^y \widetilde{W}_{kl} + \beta^4 \sum_{l=1}^{Ny+4} D_{j,l}^y \widetilde{W}_{il} + K_r \widetilde{W}_{ij} + C_r \left(\sum_{k=1}^{Nx+4} B_{i,k}^x \widetilde{W}_{kj} + \beta^2 \sum_{l=1}^{Ny+4} B_{j,l}^y \widetilde{W}_{il} \right) = \Omega^2 W_{ij}$$

$$i = 1, 2, \ldots, Nx;\ j = 1, 2, \ldots, Ny \tag{33}$$

where $D_{i,k}^x$, $D_{j,l}^y$, $B_{i,k}^y$, and $B_{j,l}^y$ are the weighting coefficients of the fourth- and second-order derivatives with respect to x or y, as calculated by Eq. (26). N_x and N_y are the numbers of grid points in the x and y directions. We chose $N_x = N_y = N$. The

Table 1
Values used for stiffness of tie bars and dowels for various boundary conditions.

	S–S–S–S edges	C–C–C–C edges	F–F–F–F edges	E–E–E–E edges
Elastic vertical restraint, *kx, ky* (N/m)	200 E + 18	200 E + 18	0	200 E + 6
Elastic rotational restraint, *krx, kry* (Nm/rad)	0	1.0 E + 18	0	1.0 E + 6
Elastic torsional restraint, *kxy* (N/m^2)	0	1.0E + 18	0	0

DOFs $\widetilde{W}_{kl}$ contain (i) the deflection W at all grid points, (ii) its second- and fourth-order derivatives with respect to x or y at all boundary points, and (iii) the mixed-order derivatives at the four corner points. There are usually $(N+4)\times(N+4)$ DOFs in total.

The governing equation is used at all $N\times N$ grid points. To ease the programming effort and maintain accuracy, the $8N+4$ degrees of freedom involving the derivatives below are considered as fictitious points out of the plate domain: $W_{,XX}(X_1,Y_j)$; $W_{,XX}(X_N,Y_j)$; $W_{,YY}(X_i,Y_1)$; $W_{,YY}(X_i,Y_N)$; $W_{,XXXX}(X_1,Y_j)$; $W_{,XXXX}(X_N,Y_j)$; $W_{,YYYY}(X_i,Y_1)$; $W_{,YYYY}(X_i,Y_N)$; $W_{,XXYY}(X_1,Y_1)$; $W_{,XXYY}(X_N,Y_1)$; $W_{,XXYY}(X_1,Y_N)$; $W_{,XXYY}(X_N,Y_N)$where $i=1, 2,\ldots, N$; $j=1, 2,\ldots, N$

It should be emphasised that these additional grid points are not the fictitious points used in Eq. (9), but were only introduced for the convenience of programming. The remaining 12 DOFs, at the corners are demonstrated to be null [8] for the isotropic and anisotropic thin-plate governing equations.

The additional degrees of freedom that appeared in Eq. (16) can be chosen differently when eliminating the fictitious points that appeared in the weighting coefficients of derivatives with different orders. As the different orders of derivatives appear in the governing equation and boundary conditions, both Eqs. (17) and (18) are used to eliminate the DOFs at the fictitious points outside the plate. The weighting coefficients of the third- and fourth-order derivatives are still calculated by Eq. (18). Instead of using Eq. (18), Eq. (17) is used to formulate the weighting coefficients of the first- and second-order derivatives, namely,

$$w^{(n)}(x_i)\approx\sum_{k=1}^{N}F_{i,k}^{(n)}w(x_k)+F_{i,N+1}^{(n)}w^{(2)}(x_1)+(0)w^{(4)}(x_1)+F_{i,N+3}^{(n)}w^{(2)}(x_N)+(0)w^{(4)}(x_N)=\sum_{k=1}^{N+4}\widetilde{F}_{i,k}^{(n)}\widetilde{w}(x_k)$$
$$i=1,2,\ldots,N;\quad and\quad n=1,2 \tag{34}$$

where $F_{i,j}^{(n)}$, N, and Δx are as defined in Eqs. (27)–(32). $\widetilde{F}_{i,k}^{(n)}$ contains all $F_{i,k}^{(n)}$; $k=1,2,\ldots,N+4$.

For convenience, the weighting coefficients of the first- to fourth-order derivatives are still denoted by $A_{i,j}$, $B_{i,j}$, $C_{i,j}$, and $D_{i,j}$. Thus, the form of the discrete governing equation remains as indicated in Eq. (33). Therefore, the total number of DOFs in Eq. (33) was reduced to N^2+8N+4. To resolve the problem, $8N+4$ boundary equations in terms of the DSC had to be added to Eq. (33). After doing so, all necessary equations were obtained. The solution procedures to obtain the frequencies are exactly the same as described in earlier studies [8,11,36].

The displacement vector can be expressed as a partitioned matrix as follows:

$$\begin{bmatrix}[K_{DD}] & [K_{DB}]\\ [K_{BD}] & [K_{BB}]\end{bmatrix}\begin{Bmatrix}\{W_D\}\\ \{W_B\}\end{Bmatrix}=\Omega^2\begin{bmatrix}[I] & [0]\\ [0] & [0]\end{bmatrix}\begin{Bmatrix}\{W_D\}\\ \{W_B\}\end{Bmatrix} \tag{35}$$

where $\{W_D\}$ contains only the displacement DOFs, its dimensions depend on the combinations of boundary conditions, and $\Omega=\omega a^2\sqrt{(\rho h+m_o)/D}$.

After eliminating $\{W_B\}$, Eq. (35) can be restored in a standard Eigenvalue matrix equation form as

$$\left[\tilde{K}\right]\{W_D\}=\Omega^2[I]\{W_D\} \tag{36}$$

Frequencies can be obtained by a standard Eigen-solver.

4. Results and discussion

To verify if the abovementioned method is applicable and can be generalised to all boundary conditions (free, F–F–F–F, clamped, C–C–C–C, simply supported, S–S–S–S and semi-rigid or elastic edges, E–E–E–E), we considered the modal properties of square and rectangular plates for several different boundary conditions. The corresponding stiffnesses of the restraining springs are specified in Table 1.

Using the procedure described above, the frequencies of an isotropic plate resting on an elastic Modified Vlasov foundation were analysed. A finite rectangular plate of 3.5m × 5m × 0.25m, dowelled along its edges, was considered as shown in Fig. 1. The structural properties of the plate were density $\rho=2500\text{kgm}^{-3}$, Poisson's ratio $\upsilon=0.25$, and longitudinal elastic modulus $E=24\times10^9\text{Pa}$. The density of the subgrade was $m_s=1800\text{kgm}^{-3}$, Poisson's ratio $\upsilon_S=0.35$, and longitudinal elastic modulus $E_S=50.10^6\text{Pa}$.

4.1. Convergence study

A convergence study of the method is conducted for lower- and higher-frequency modes using the S–S–S–S boundary conditions and $k_o=c_o=0$. For this purpose, we considered N = 11, 19, 25, and 33 points of the grid. As the number of

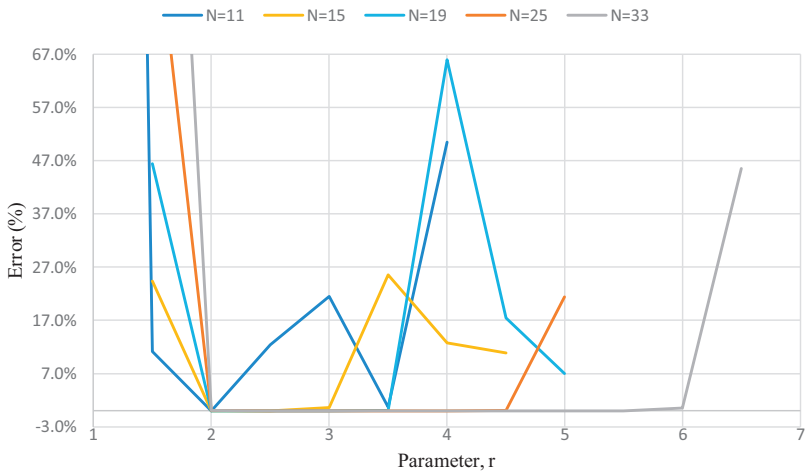

Fig. 2(a). Percentage of relative errors of DSC-T-A data for exact solutions (S–S–S–S) as a function of parameter r for various numbers of grid points in first mode.

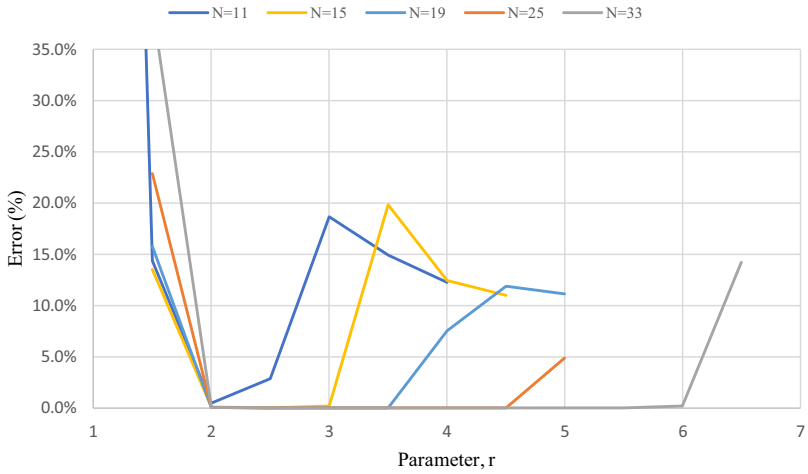

Fig. 2(b). Percentage of relative errors of DSC-T-A data for exact solutions (S–S–S–S) as a function of parameter r for various numbers of grid points in 10th mode.

Table 2
Values of parameter r allowing to obtain good precision (error $<$ 1%) according to different numbers of grid points.

	$N=11$	$N=15$	$N=19$	$N=25$	$N=33$
Mode 1	2.0 and 3.5	[2 ; 3.0]	[2 ; 3.5]	[2 ; 4.5]	[2 ; 6.0]
Mode 10	2.0	[2 ; 3.0]	[2 ; 3.5]	[2 ; 4.5]	[2 ; 6.0]
Mode 75	–	[3.5 ; 4.0]	[2.5 ; 4.0]	[2 ; 5.0]	[2 ; 6.0]
Mode 150	–	–	[4.0 ; 5.0]	$\geq$ 3.5	$\geq$ 2.5
Mode 280	–	–	–	–	$\geq$ 3.5
Mode 500	–	–	–	–	$\geq$ 5.0

grid points must be accompanied by the adjustment of the r parameter involved in the DSC-RSK method, the convergence study consisted of determining from which number of grid points and for which interval of values of r the program uses, stabilises, and converges. The curves in Figs. 2(a)–2(f) show the relative errors of the method for the frequency value of different modes as a function of parameter r and the number of grid points. These curves are plotted for the numbers of modes 1, 10, 75, 150, 280, and 500.

Note that when the number of grid points is low, the range of values of parameter r to obtain a good accuracy ($<$1%) is also small. For example, for N = 11 and 15, we have good precision only for lower modes, while for N = 19, 25, and 33, we have precise frequencies for both lower modes and higher modes. In addition, the higher the number of grid points, the higher the number of accurately calculable modes. Table 2 summarises the intervals in which it is necessary to choose r to obtain good precision (error $<$ 1%) according to the mode and the number N in the case of the studied problem.

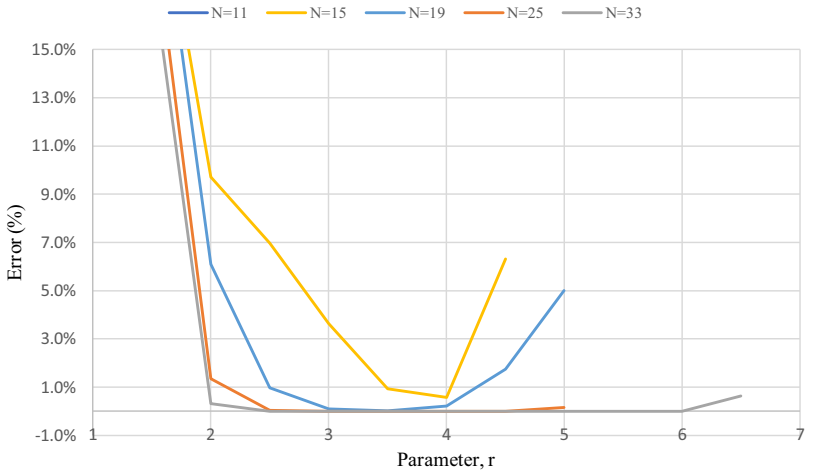

Fig. 2(c). Percentage of relative errors of DSC-T-A data for exact solutions (S–S–S–S) as a function of parameter *r* for various numbers of grid points in 75th mode.

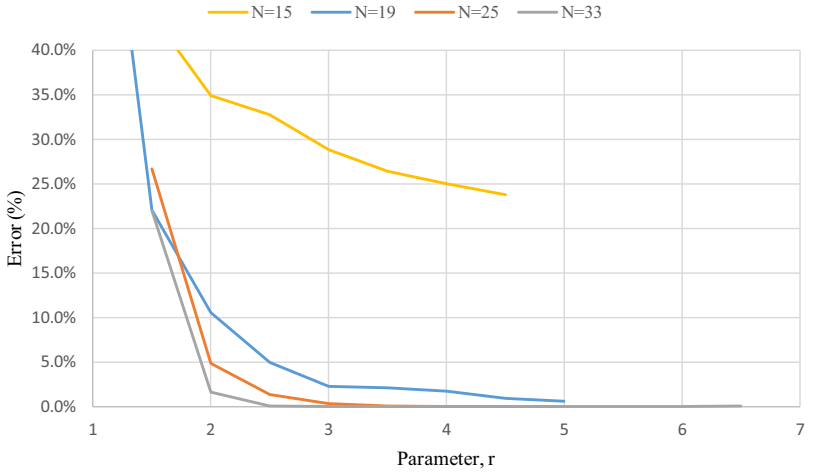

Fig. 2(d). Percentage of relative errors of DSC-T-A data for exact solutions (S–S–S–S) as a function of parameter *r* for various numbers of grid points in 150th mode.

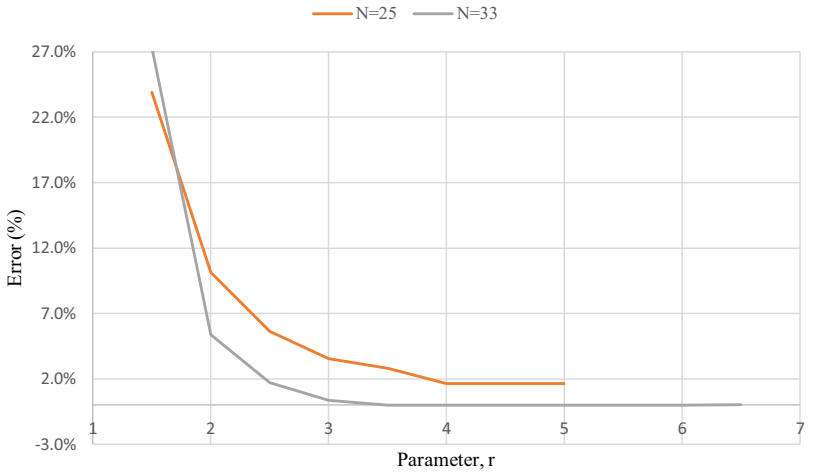

Fig. 2(e). Percentage of relative errors of DSC-T-A data for exact solutions (S–S–S–S) as a function of parameter *r* for various numbers of grid points in 280th mode.

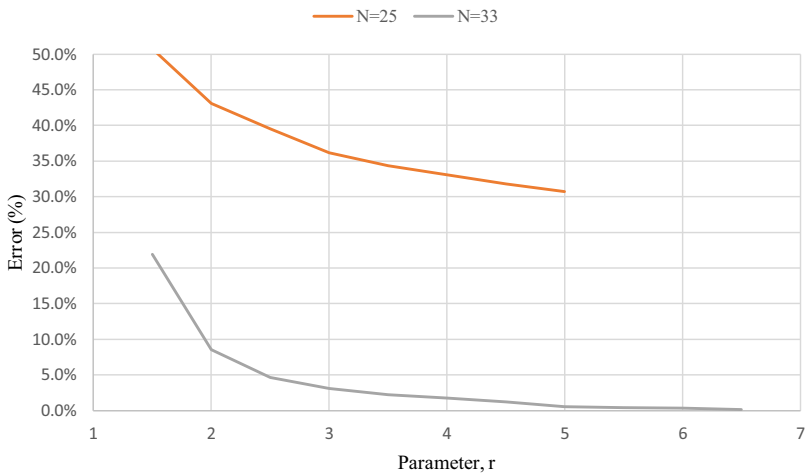

Fig. 2(f). Percentage of relative errors of DSC-T-A data for exact solutions (S–S–S–S) as a function of parameter r for various numbers of grid points in 500th mode.

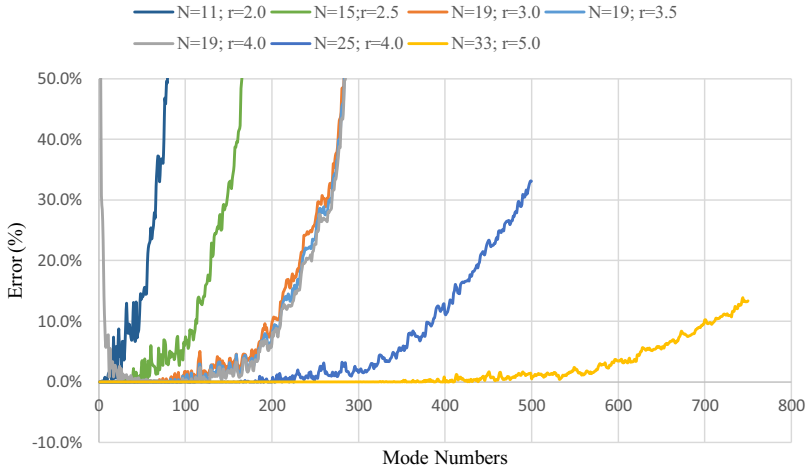

Fig. 3. Percentage of relative errors of DSC-T-A data for exact solutions (S–S–S–S) as a function of mode numbers for various pairs (N, r).

To have the frequencies of the higher modes, it is necessary to have high numbers of grid points. Therefore, one could deduce that the ranges of the values of parameter r to be used for the implementation vary according to the number of grid points and depend on whether one is studying the lower or higher modes.

For a better appreciation of the convergence of the method for the lower and higher modes, we plotted the curves for variation of the relative error on the values of the frequencies as a function of the number of modes (Fig. 3). To do so, we based the results of the convergence study on a simply supported plate to choose the best couples (N, r) if the controllable parameter r is chosen appropriately.

Fig. 3 shows that for lower modes, the low values of N are sufficient. For example, for $N = 19$, we can have precise frequencies up to 150 modes. Moreover, for $N = 33$, this graph shows that this method can accurately calculate frequencies for higher-mode numbers (up to 550 modes for $N = 33$) without losing precision for lower modes.

4.2. Applicability of used method to case of semi-rigid boundary conditions

To verify the present procedure, a plate with elastic boundary conditions was used. The ordinary boundary conditions can be obtained from Table 1. The results were compared with those of other studies and those of symmetric and antisymmetric extensions, as in Table 3.

For S–S–S–S, the result of the current approach is close to that of an exact solution, and the average relative error percentage is 10^{-7}. For the C–C–C–C boundary condition, the vibration obtained by asymptotic input stiffness according to Table 1 is accurate enough with an average relative difference of 0.07%. By cancelling the rigidities in Table 1, the values indicated under column F–F–F–F in Table 3, are obtained, and are the same boundary conditions as indicated in prior

Table 3
Natural frequencies of isotropic thin square plate with various types of boundary conditions and without soil [$k_0 = 0$; $c_0 = 0$; $N = 19$; $M = 18$; $\upsilon = 0.3$; $\sigma = 3.0 \times \Delta$].

Mode number	S–S–S–S		C–C–C–C		F–F–F–F	
	Authors' approach	Exact method	Authors' approach	Leissa [41] Wang and Xu [24] Liu and Banerjee [42]	Authors' approach	Leissa [41] Wang and Xu [24] Wang et al. [15]
1	19.739162	19.739207	35.9806	35.992 35.986 35.9852	13.465445	13.489 13.419 13.468
2	49.348022	49.348022	73.4275	73.413 73.399 73.3938	19.595261	19.789 19.559 19.596
3	49.348022	49.348022	73.4275	73.413 73.400 73.3938	24.270666	24.432 24.212 24.270
4	78.956847	78.956836	108.195	108.27 108.23 108.217	34.793873	35.024 34.646 34.802
5	98.696035	98.696044	131.54	131.64 131.57 131.581	34.793873	35.024 34.646 34.802
6	98.696035	98.696044	132.138	132.24 132.22 132.205	61.091408	61.526 60.878 61.257
7	128.30486	128.30486	164.636	– – 165.000	61.091408	– – –
8	128.30486	128.30486	164.834	– – 165.000	63.664099	– – –
9	167.78327	167.78328	210.388	– – –	69.24159	– – –
10	167.78327	167.78328	210.496	– –	77.165036	– –

studies [8]. The obtained results sufficiently demonstrate the applicability of the proposed method as the relative difference is less than 0.07%. This is a significant precision for the dynamic modelling of civil engineering structures, especially for pavement plates. This resolution approach using semi-rigid boundary conditions (E–E–E–E) can be used for any other type of boundary conditions of a pavement plate, with the same calculation code and without precision loss.

4.3. Effect of Modified Vlasov soil type on free vibration of rectangular plate

Table 4 lists the free vibrations of a plate resting on a Modified Vlasov foundation for various boundary conditions. k_0 and $c_0$are different from zero. The stiffness owing to the surrounding soil effect on the boundaries of the plate is omitted, as in the case of the Vlasov soil type. The results of this system are useful for comparison. Comparing the results of the Taylor series expansion approach obtained by asymptotic values of stiffness (DSC-T-A), symmetric (DSC-S), and anti-symmetric (DSC-A) extensions, we noticed that the DSC-T-A approach led to accurate results. For both C–C–C–C plates, the same result is observed, with and without considering the surrounding soil stiffness. This can be explained by the fact that for C–C–C–C, both the rotational and translational stiffness were assumed to be infinite. Thus, a finite value added to the edge stiffness was insignificant.

Given the results of S–S–S–S, corresponding to the case when the stiffness of the surrounding soil was not considered and the case when it was considered, the average difference was almost negligible at less than 0.14%. As the elastic vertical translational stiffness is infinite, it can be concluded that the rotational rigidity of the surrounding soil has a negligible effect. Analysing the case of F–F–F–F, the average difference between the case when the stiffness of the surrounding soil was not considered and the case when it was considered was 17%. However, this difference increases as the number of modes increases. This leads to the conclusion that the elastic vertical translational stiffness has a significant effect on the values of the frequencies of the plates, particularly for high frequencies. Neglecting the translational stiffness of the surrounding soil can lead to significant errors in the modelling of the plate, especially in the free vibration analysis of free edges and elastic boundary conditions.

Table 4
Natural frequency of isotropic thin rectangular plates resting on a Modified Vlasov soil type [$a = 5$m;$b = 3.5$m;$N = 19$; $M = 18$;$\sigma = 3.0\Delta$; $\upsilon = 0.25$; $H_S = 1.5$m; $\gamma = 4.212$].

Mode number	Results when the stiffness of the surrounding soil was not considered					Results when the stiffness of the surrounding soil was considered				
	S–S–S–S		C–C–C–C		F–F–F–F	S–S–S–S		C–C–C–C		F–F–F–F
	DSC-T-A	DSC-A	DSC-T-A	DSC-S		DSC-T-A	DSC-A	DSC-T-A	DSC-S	
1	55.6165	55.641	73.412	73.4522	50.2612	55.4624	–	73.3536	–	48,6925
2	76.3809	76.3073	102.075	102.102	51.1704	76.4834	–	101.759	–	52,0026
3	102.645	102.583	144.532	144.584	65.2457	102.947	–	144.371	–	53,47
4	119.363	119.432	154.417	154.639	65.3339	119.671	–	154.909	–	58,9678
5	129.668	129.724	174.283	174.605	74.0473	129.548	–	174.842	–	59,2015
6	176.725	176.73	226.009	226.422	79.5715	176.893	–	225.526	–	72,9668
7	185.126	185.105	229.58	229.944	97.6029	185.083	–	229.274	–	73,5749
8	197.84	197.813	261.781	262.036	106.55	197.925	–	261.739	–	80,8052
9	226.624	226.713	291.56	292.097	129.648	226.806	–	291.556	–	86,2866
10	244.121	244.096	299.279	300.243	133.659	244.189	–	299.519	–	103,708

Table 5
Natural frequency for the first ten modes as a function of the aspect ratio β and the dynamically activated depth of the Modified Vlasov soil type when all edges of the plate were elastically restrained (E–E–E–E) [$h = 0.25$m;$E = 24.10^9$Pa;$\upsilon = 0.25$;$N = 19$; $M = 18$; $\sigma = 3.0\Delta$].

H_s	γ	Ratio β	Mode 1	Mode 2	Mode 3	Mode 4	Mode 5	Mode 6	Mode 7	Mode 8	Mode 9	Mode 10
0,5	1493	1	59.8992	70.8612	70.8612	83.1214	92.5545	94.2738	104.943	104.943	122.691	122.691
		0,7	30.7314	36.2982	42.3371	47.1487	47.7888	57.6713	59.4674	60.7334	65.5087	71.7442
		0,5	17.1785	19.9263	25.212	26.3636	28.944	32.0441	33.7781	39.5644	41.2348	42.239
		0,3	7.68156	8.45248	10.0793	12.2695	12.3098	13.3808	15.5874	15.6472	19.079	21.0778
		0,1	1.3508	1.39741	1.51858	1.705	2.00715	2.30498	2.53789	2.69185	3.34024	3.56476
1	2.832	1	50.9026	63.5267	63.5267	77.0172	87.1101	88.9446	100.209	100.209	118.661	118.661
		0,7	26.5709	32.887	39.4573	44.5957	45.2748	55.6185	57.4581	58.7822	63.703	70.1165
		0,5	15.275	18.3253	23.9749	25.1707	27.8694	31.0835	32.8691	38.7885	40.5018	41.5248
		0,3	7.14249	7.9698	9.68045	11.9377	11.9863	13.0793	15.3325	15.3981	18.8753	20.9005
		0,1	1.31342	1.36165	1.48598	1.67614	1.98306	2.28318	2.51953	2.67331	3.32699	3.55101
1,5	4.212	1	49.8423	62.6946	62.6946	76.3409	86.5122	88.3606	99.6958	99.6958	118.227	118.227
		0,7	26.0867	32.503	39.1387	44.3164	45.0003	55.3973	57.2407	58.572	63.509	69.943
		0,5	15.0577	18.147	23.8402	25.0404	27.7529	30.9802	32.7716	38.7054	40.4241	41.4492
		0,3	7.0826	7.91683	9.63727	11.9017	11.9516	13.0468	15.3053	15.3718	18.8538	20.8822
		0,1	1.30935	1.35779	1.48247	1.67305	1.98051	2.28083	2.51763	2.67132	3.32566	3.54955
2	5.611	1	49.7442	62.6182	62.6182	76.279	86.4575	88.3072	99.6489	99.6489	118.187	118.187
		0,7	26.042	32.4677	39.1095	44.2909	44.9752	55.3771	57.2209	58.5529	63.4913	69.9273
		0,5	15.0377	18.1306	23.8279	25.0285	27.7423	30.9708	32.7628	38.6979	40.417	41.4423
		0,3	7.07711	7.91199	9.63333	11.8984	11.9484	13.0438	15.3028	15.3694	18.8519	20.8806
		0,1	1.30898	1.35743	1.48215	1.67276	1.98028	2.28062	2.51746	2.67114	3.32555	3.54941
2,5	7.016	1	49.7446	62.6184	62.6184	76.2792	86.4577	88.3074	99.6491	99.6491	118.187	118.187
		0,7	26.0422	32.4679	39.1096	44.291	44.9753	55.3772	57.2209	58.5529	63.4914	69.9273
		0,5	15.0378	18.1307	23.8279	25.0286	27.7423	30.9708	32.7628	38.6979	40.417	41.4423
		0,3	7.07713	7.912	9.63334	11.8985	11.9484	13.0438	15.3028	15.3694	18.8519	20.8806
		0,1	1.30898	1.35743	1.48215	1.67277	1.98028	2.28062	2.51746	2.67114	3.32555	3.54941
3	8.418	1	49.7412	62.6158	62.6158	76.277	86.4558	88.3055	99.6474	99.6474	118.186	118.186
		0,7	26.0406	32.4666	39.1086	44.2901	44.9744	55.3765	57.2202	58.5523	63.4908	69.9267
		0,5	15.0371	18.1301	23.8275	25.0281	27.742	30.9705	32.7625	38.6976	40.4168	41.4421
		0,3	7.07694	7.91183	9.63321	11.8983	11.9483	13.0437	15.3028	15.3694	18.8518	20.8805
		0,1	1.30897	1.35742	1.48214	1.67276	1.98027	2.28061	2.51745	2.67113	3.32554	3.54941

4.4. Parametric study of free vibration analysis

Table 5 presents the natural frequencies as function of the aspect ratio ($\beta = a/b$) and the dynamically activated depth H_S of the Modified Vlasov soil type when all edges of the plate were elastically restrained (E–E–E–E). From the calculations made during the study, we found that the plate with $\beta = a/b$ and the plate with $\beta = b/a$ had the same dimensional frequencies. For semi-rigid boundary conditions, the aspect ratio affected the dimensionless frequencies, as shown in Table 5. For example, for the first mode, the frequencies vary from 59.8992 for $\beta = 1$ to 1.3508 for $\beta = 0.1$. Thus, the frequencies increase when the plate aspect ratio increases. This trend was also observed in prior studies in the field [2,31]. In addition, it is noted that for the square plate ($\beta = 1$), the consecutive frequencies of modes 2 and 3 and modes 7 and 8 are equal. On the other hand, for rectangular plates ($\beta \neq 1$), certain consecutive frequencies (for example, those of modes 4 and 5

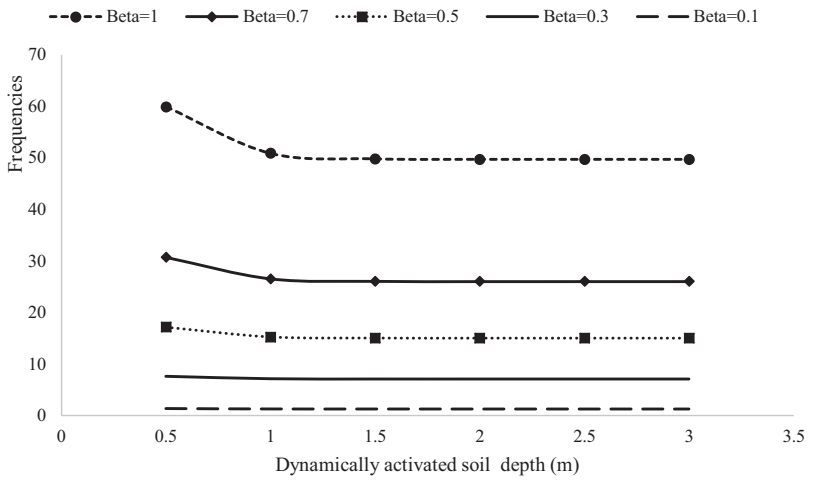

Fig. 4. Natural frequency variation as a function of dynamically activated soil depth H_S for various aspect ratio β.

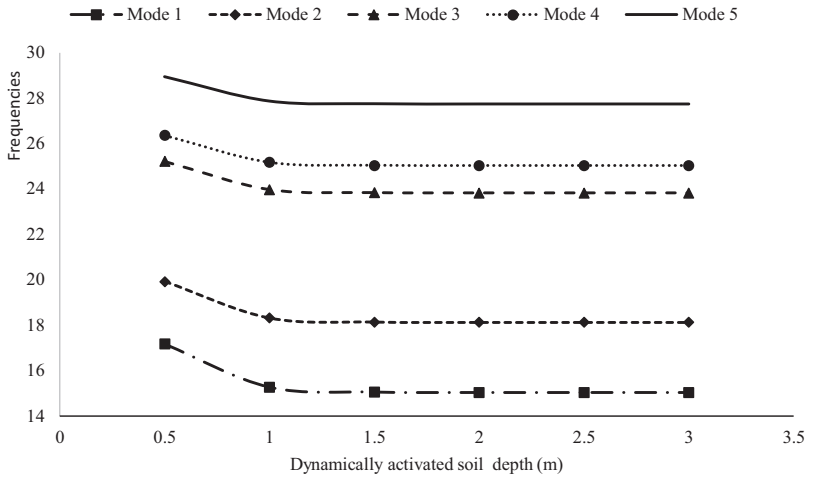

Fig. 5. Natural frequency variation as a function of dynamically activated soil depth H_S for first five mode numbers and for $\beta = 0.5$.

for $\beta = 0.7$ and modes 7 and 8 for $\beta = 0.3$) are sufficiently close to one of the other. The consecutive similar modes can be understood like the values of frequencies corresponding to the modes with half-wave numbers (m,n) and (n,m).

Fig. 4 shows that for $\beta = 0.1$ and $\beta = 0.3$, frequency values vary little, as the depth H_S increases at an average of less than 6%. The opposite is true for $\beta = 0.5$, 0.7, 1.0, with an average of more than 17%. This could mean that the natural frequency values are more influenced by the depth H_S if the shape of the plate tends to be square. Therefore, the soil depth H_S influences the frequency values of the plates more than the beams.

Figs. 4 and 5 show that for soil depths of more than $H_S = 1.5$m, the frequencies were almost constant. This was noted for all mode numbers and was also discussed in [4], which studied the case of a deflection analysis on the Vlasov soil type. The same trend was observed for free vibrations, but the considered soil was the Vlasov type [2]. This means that beyond a certain depth of soil, the frequency does not vary. Thus, the soil below this depth has no effect on the response of the plate. In this study, the soil was considered to have a depth of $H_S = 1.5$m and was assumed to be resting on a rigid substratum.

5. Conclusions

The influence of the stiffness of a surrounding Modified Vlasov soil type, soil depth, and aspect ratio on the free vibration of a thin rectangular plate whose edges are semi-rigid is successfully analysed by a DSC using the Taylor series expansion method. The two formulas of the Taylor series expansion are used in the DSC to eliminate the fictitious points outside the physical domain. In this way, the difficulty in applying the boundary conditions at corner points by a DSC with a Taylor series expansion is tackled by specifying the value of the torsional stiffness at the corners. Some test examples have been studied to demonstrate the convergence properties and accuracy of the proposed DSC-T method for lower and higher

modes. The effects of the controllable parameter r are studied. It is shown that parameter r influences the convergence and accuracy of the method.

The main conclusions of this study are as follows:

(i) Beyond a certain depth, the effective depth of soil and frequency do not vary consistently.
(ii) The dynamically activated depth influences the frequency values for plates more than for beams.
(iii) The effect of the elastic rotational stiffness of the surrounding soil is found to be negligible compared to that of the elastic vertical translational one.
(iv) Based on the results reported herein, the proposed DSC method with two different formulas of Taylor series expansion to eliminate the fictitious points outside the physical domain of the plate led to accurate frequencies for a plate with semi-rigid boundary conditions.
(v) With the proposed DSC method, it is possible by varying the plate edge stiffness to use the same calculation program for all boundary conditions.

The numerical results showed that we can calculate the accurate values of the frequencies of a dowelled rectangular thin isotropic plate resting on a Modified Vlasov soil type using the present approach. This study can serve as a basis for the dynamic analysis of rectangular plates compared to other parameters such as the study of deflection.

References

[1] Q. Zhu, X. Wang, Free vibration analysis of thin isotropic and anisotropic rectangular plates by the discrete singular convolution algorithm, Int. J. Numer. Methods Eng. 86 (2011) 782–800, doi:10.1002/nme.
[2] K. Ozgan, A.T. Daloglu, Free vibration analysis of thick plates on elastic foundations using modified Vlasov model with higher order finite elements, Indian J. Eng. Mater. Sci. 19 (2012) 279–291.
[3] S.W. Alisjahbana, W. Wangsadinata, Dynamic analysis of rigid roadway pavement under moving traffic loads with variable velocity, Interact. Multiscale Mech. 5 (2012) 105–114, doi:10.12989/imm.2012.5.2.105.
[4] M. Gibigaye, C.P. Yabi, I.E. Alloba, Dynamic response of a rigid pavement plate based on an inertial soil, Int. Sch. Res. Not. (2016), doi:10.1155/2016/4975345.
[5] H. Khov, W.L. Li, R.F. Gibson, An accurate solution method for the static and dynamic deflections of orthotropic plates with general boundary conditions, Compos. Struct. 90 (2009) 474–481, doi:10.1016/j.compstruct.2009.04.020.
[6] S.W. Alisjahbana, S. Sumawiganda, S. Leman, Dynamic of rigid roadway pavement under dynamic loads dynamic of rigid roadway pavement under dynamic, in: Proceedings of the Thirty-fourth Conference on Our World Concrete and Structures, 2009.
[7] P. Pevzner, T. Weller, A. Berkovits, Further modification of bolotin method in vibration analysis, AIAA J. 38 (2000) 1725–1729, doi:10.2514/2.1159 A.
[8] X. Wang, Z. Yuan, Discrete singular convolution and Taylor series expansion method for free vibration analysis of beams and rectangular plates with free boundaries, Int. J. Mech. Sci. 122 (2017) 184–191, doi:10.1016/j.ijmecsci.2017.01.023.
[9] F. Tornabene, N. Fantuzzi, F. Ubertini, E. Viola, Strong formulation finite element method based on differential quadrature: a survey, Appl. Mech. Rev. 67 (2015) 20801-1–20801-55, doi:10.1115/1.4028859.
[10] S.Y. Yang, Y.C. Zhou, G.W. Wei, Comparison of the discrete singular convolution algorithm and the Fourier pseudospectral method for solving partial differential equations, Comput. Phys. Commun. 143 (2002) 113–135, doi:10.1016/S0010-4655(01)00427-1.
[11] C.W. Bert, X. Wang, A.G. Striz, Differential quadrature for static and free vibration analyses of anisotropic plates, Int. J. Solids Struct. 30 (1993) 1737–1744, doi:10.1016/0020-7683(93)90230-5.
[12] X. Wang, Y. Wang, R. Chen, Static and free vibrational analysis of rectangular plates by the differential quadrature element method, Commun. Numer. Methods Eng. 1141 (1998) 1133–1141 12<1133::AID-CNM213>3.0.CO;2-Q, doi:10.1002/(SICI)1099-0887(199812)14.
[13] C. Shu, Q. Yao, K.S. Yeo, Block-marching in time with DQ discretization: An efficient method for time-dependent problems, Comput. Methods Appl. Mech. Eng. 191 (2002) 4587–4597, doi:10.1016/S0045-7825(02)00387-0.
[14] C. Shu, C.M. Wang, Treatment of mixed and nonuniform boundary conditions in GDQ vibration analysis of rectangular plates, Eng. Struct. 21 (1999) 125–134, doi:10.1016/S0141-0296(97)00155-7.
[15] Y. Wang, X. Wang, Y. Zhou, Static and free vibration analyses of rectangular plates by the new version of the differential quadrature element method, Int. J. Numer. Methods Eng. 59 (2004) 1207–1226, doi:10.1002/nme.913.
[16] C.H.W. Ng, Y.B. Zhao, Y. Xiang, G.W. Wei, On the accuracy and stability of a variety of differential quadrature formulations for the vibration analysis of beams, Int. J. Eng. Appl. Sci. 1 (2009) 1–25. http://ink.library.smu.edu.sg/lkcsb_research/1708/.
[17] A. Fereidoon, M. Asghardokht Seyedmahalle, A. Mohyeddin, Bending analysis of thin functionally graded plates using generalized differential quadrature method, Arch. Appl. Mech. 81 (2011) 1523–1539, doi:10.1007/s00419-010-0499-3.
[18] H. Zhong, T. Yu, A weak form quadrature element method for plane elasticity problems, Appl. Math. Model. 33 (2009) 3801–3814, doi:10.1016/j.apm.2008.12.007.
[19] Leissa, A.W. Leissa, Vibration of plates, NASA SP-160, Washington D.C., 1969.
[20] Y.B. Zhao, G.W. Wei, DSC analysis of rectangular plates with non-uniform boundary conditions, J. Sound Vib. 255 (2002) 203–228, doi:10.1006/jsvi.2001.4150.
[21] G.W. Wei, Y.B. Zhao, Y. Xiang, A novel approach for the analysis of high-frequency vibrations, J. Sound Vib. 257 (2002) 207–246, doi:10.1006/jsvi.5055.
[22] D. Wang, J.J. Gino, Detailed comparison of numerical methods for the perturbed sine-Gordon equation with impulsive forcing, J. Eng. Math. (2014), doi:10.1007/s10665-013-9678-x.
[23] O. Civalek, Analysis of thick rectangular plates with symmetric cross-ply laminates based on first-order shear deformation theory, J. Compos. Mater. 42 (2008) 2853–2867, doi:10.1177/0021998308096952.
[24] X. Wang, S. Xu, Free vibration analysis of beams and rectangular plates with free edges by the discrete singular convolution, J. Sound Vib. 329 (2010) 1780–1792, doi:10.1016/j.jsv.2009.12.006.
[25] G.W. Wei, Discrete singular convolution for the solution of the Fokker–Planck equation, J. Chem. Phys. 110 (1999) 8930–8942, doi:10.1063/1.478812.
[26] O. Civalek, A. Korkmaz, Ç. Demir, Discrete singular convolution approach for buckling analysis of rectangular Kirchhoff plates subjected to compressive loads on two-opposite edges, Adv. Eng. Softw. 41 (2010) 557–560, doi:10.1016/j.advengsoft.2009.11.002.
[27] O. Civalek, Fundamental frequency of isotropic and orthotropic rectangular plates with linearly varying thickness by discrete singular convolution method, Appl. Math. Model. 33 (2009) 3825–3835, doi:10.1016/j.apm.2008.12.019.
[28] O. Civalek, A. Yavas, Large deflection static analysis of rectangular plates on two parameter elastic foundations, Int. J. Sci. Technol. 1 (2006) 43–50 10.1.1.530.5332.
[29] S. Zhao, G.W. Wei, Y. Xiang, DSC analysis of free-edged beams by an iteratively matched boundary method, J. Sound Vib. 284 (2005) 487–493, doi:10.1016/j.jsv.2004.08.037.
[30] M. Huang, X.Q. Ma, T. Sakiyama, H. Matsuda, C. Morita, Free vibration analysis of square plates resting on non-homogeneous elastic foundations, J. Appl. Mech. 7 (2004) 225–232, doi:10.2208/journalam.7.225.

[31] H. Matsunaga, Vibrations and stability of thick plates on elastic foundations, J. Eng. Mech. 126 (2000) 27–34, doi:10.1061/(ASCE)0733-9399(2000)126:1(27).
[32] H. Zhong, X. Li, Y. He, Static flexural analysis of elliptic Reissner–Mindlin plates on a Pasternak foundation by the triangular differential quadrature method, Arch. Appl. Mech. 74 (2005) 679–691, doi:10.1007/s00419-005-0377-6.
[33] A. Turhan, A Consistent Vlassov Model for Analysis of Plates on Elastic Foundations Using Finite Element Method, Texas Technologie University, 1992.
[34] X. Wang, Y. Wang, S. Xu, DSC analysis of a simply supported anisotropic rectangular plate, Compos. Struct. 94 (2012) 2576–2584, doi:10.1016/j.compstruct.2012.03.005.
[35] A.K. Baltacioglu, B. Akgoz, O. Civalek, Nonlinear static response of laminated composite plates by discrete singular convolution method, Compos. Struct. 93 (2010) 153–161, doi:10.1016/j.compstruct.2010.06.005.
[36] O. Civalek, Nonlinear analysis of thin rectangular plates on Winkler–Pasternak elastic foundations by DSC–HDQ methods, Appl. Math. Model. 31 (2007) 606–624, doi:10.1016/j.apm.2005.11.023.
[37] G.W. Wei, Y.B. Zhao, Y. Xiang, Discrete singular convolution and its application to the analysis of plates with internal supports. Part 1: theory and algorithm, Int. J. Numer. Methods Eng. 55 (2002) 913–946, doi:10.1002/nme.527.
[38] Y.B. Zhao, G.W. Wei, Y. Xiang, Discrete singular convolution for the prediction of high frequency vibration of plates, Int. J. Solids Struct. 39 (2001) 65–88, doi:10.1016/S0020-7683(01)00183-4.
[39] G. Duan, X. Wang, Vibration analysis of stepped rectangular plates by the discrete singular convolution algorithm, Int. J. Mech. Sci. 82 (2014) 100–109, doi:10.1016/j.ijmecsci.2014.03.004.
[40] S. Xu, X. Wang, Free vibration analyses of Timoshenko beams with free edges by using the discrete singular convolution, Adv. Eng. Softw. 42 (2011) 797–806, doi:10.1016/j.advengsoft.2011.05.019.
[41] A.W. Leissa, The free vibration of rectangular plates, J. Sound Vib. 31 (1973) 257–293, doi:10.1016/S0022-460X(73)80371-2.
[42] X. Liu, J.R. Banerjee, Free vibration analysis for plates with arbitrary boundary conditions using a novel spectral-dynamic stiffness method, Comput. Struct. 164 (2016) 108–126, doi:10.1016/j.compstruc.2015.11.005.